Ultrasound in Medicine & Biology 51 (2025) 373–380

Contents lists available at ScienceDirect

Ultrasound in Medicine & Biology

journal homepage: www.elsevier.com/locate/ultrasmedbio

Original Contribution

Effects of Different Gas Cores on the Ambient Pressure Sensitivity of the Subharmonic Response of SonoVue

Roozbeh H. Azami [a], Mehmet Yapar [a], Saikat Halder [a], Flemming Forsberg [b], John R. Eisenbrey [b], Kausik Sarkar [a,*]

[a] Department of Mechanical and Aerospace Engineering, The George Washington University, Washington, DC, USA
[b] Department of Radiology, Thomas Jefferson University, Philadelphia, PA, USA

ARTICLE INFO

Keywords:
Ambient pressure sensitivity
Subharmonic aided pressure estimation (SHAPE)
Ultrasound contrast agents
SonoVue
Sulfur hexafluoride
Perfluorobutane
Lumason

ABSTRACT

Objective: Subharmonic Aided Pressure Estimation (SHAPE) is a noninvasive technique for estimating organ-level blood pressure using the strong correlation between the subharmonic signal and ambient pressure. The compressible gas core of microbubbles enables them to generate linear and nonlinear acoustic responses when exposed to ultrasound. Here, the sulfur hexafluoride (SF_6) gas core of SonoVue (known as Lumason in the United States), a clinical contrast agent, was exchanged with a perfluorobutane (PFB) core to investigate its effect on the SHAPE response.
Methods: Excitations of 25–700 kPa peak negative pressure (PNP) and 3 MHz transmission frequency were used to study *in vitro* the effects of overpressure changes ranging from 5 to 25 kPa (37–186 mm Hg).
Results: Unlike SonoVue with SF_6, at low PNPs (<400 kPa), SonoVue with a PFB gas core exhibited no subharmonic at the atmospheric pressure, but during pressurization, a stable subharmonic response (maximum of 25 dB at 100 kPa PNP and 20 kPa Overpressure) appeared. SonoVue with a PFB gas core showed an increase in subharmonics with overpressure at high PNPs (>400 kPa), which was not observed before in normal SonoVue or other lipid microbubbles. With negligible size distribution difference between these two microbubbles, these effects on subharmonic generation are likely due to the gas core, casting new light on the mechanism by which ambient overpressure affects subharmonic.
Conclusion: This study may inform future SHAPE technique developments.

Introduction

Microbubbles with a diameter ranging between 1 and 8 μm comprising a nanometer-thick shell of lipid, protein, or polymer encapsulating a gas core serve as contrast agents in ultrasound imaging [1–3]. Thanks to their compressible gas core, these microspheres undergo volume oscillations when exposed to ultrasound. At large amplitude ultrasound excitations, bubbles scatter various nonlinear acoustic waves in addition to the linear fundamental oscillation at the same frequency of the excitation [4–6]. The nonlinear response of bubbles has been utilized in various advanced therapeutic and diagnostic applications [7–14]. Among those is the subharmonic aided pressure estimation (SHAPE) technique, which utilizes the strong correlation between ambient pressure and the subharmonic response of bubbles, happening at half the excitation frequency, to estimate the local fluid pressure inside blood vessels and organs noninvasively [15–20]. In this study, we investigate the role of the gas core of a contrast agent on the subharmonic response and ambient pressure sensitivity of SonoVue (a.k.a. Lumason in the United States; Bracco Diagnostics, Princeton, NJ, USA) by replacing the SF_6 gas core with perfluorobutane (PFB).

Acoustic excitation amplitudes larger than a threshold value are needed for bubbles to generate a subharmonic response. While typically subharmonic generation shows three stages of occurrence (at threshold), growth, and saturation, with the latter two happening beyond an approximately 200–500 kPa peak negative pressure threshold [21–25], some studies reported significantly lower thresholds at about 50 kPa [26–29]. Most of them are for SonoVue agent with its SF_6 gas core instead of bubbles with more common perfluorocarbon indicating a critical role of the gas core. Our previous study [30] showed that SonoVue bubbles produce subharmonic at PNPs as low as 25 kPa followed by two separate phases of growth and saturation with increasing PNP. A similar subharmonic profile was reported by Xu et al. [27] as well, whereas a tri-phasic behavior has been reported in other studies [29,31]. The subharmonic generated at low (≤400 kPa) and high (>400 kPa) excitations for

* Corresponding author. The George Washington University, 800 22nd Street NW, Suite 3000, Washington, DC 20052, USA
E-mail address: sarkar@gwu.edu (K. Sarkar).

https://doi.org/10.1016/j.ultrasmedbio.2024.11.006
Received 26 August 2024; Revised 15 October 2024; Accepted 4 November 2024

Table 1
Subharmonic Sensitivity Coefficients and R^2 Values for SonoVuePFB and SonoVue in 0–20 *kPa* (0–150 mm Hg) Overpressure Interval

	SonoVuePFB		*SonoVue*	
PNP (*kPa*)	Sensitivity Coefficients (dB/ mm Hg)	R^2	Sensitivity Coefficients (dB/ mm Hg)	R^2
25	0.100	0.858	-0.048	0.719
50	0.146	0.964	-0.047	0.764
100	0.158	0.924	-0.070	0.901
200	0.149	0.930	-0.055	0.728
300	0.142	0.925	-0.049	0.617
400	0.111	0.865	-0.041	0.617
500	0.041	0.784	-0.055	0.711
600	0.033	0.615	-0.040	0.537
700	0.031	0.544	-0.029	0.654

SonoVue (named Type I and II, respectively) behaved differently. Note that the transition excitation (~400 kPa PNP) observed for a 32-cycle, 3 MHz excitation might change for different excitation parameters.

The sensitivity of subharmonic signals to ambient pressure was shown to differ depending on the excitation parameters (Table 1 in Azami et al. [32]). To address contradicting reports on subharmonic correlation—both positive and negative—with ambient pressure, in our previous study we studied the effect of an increase in hydrostatic pressure on the subharmonic amplitude over a wide range of PNPs covering all stages of subharmonic production [32]. For a lipid bubble with a C_4F_{10} gas core with its typical three stages of subharmonic (occurrence, growth, saturation), adding overpressure resulted in a subharmonic decrease at the growth and saturation stage. The linear decrease in subharmonic with overpressure in the growth stage is the current standard method used in SHAPE because of both strong sensitivity and the high subharmonic amplitude, which is detectable with a clinical scanner [33]. On the other hand, increasing overpressure triggered and increased subharmonic signal levels for PNP values for which the baseline subharmonic at atmospheric pressure is close to the noise level. This observation, which was in accordance with Frinking et al. [28] partially addressed the contradictory trends in ambient pressure sensitivity measurements in the literature. Forcing bubbles into a buckling stage by elevated hydrostatic pressure rather than the acoustic pressure was responsible for the subharmonic increase at low excitation amplitudes. It is worth noting however that Mayer et al. [31] did not detect any subharmonic activities with overpressure below threshold (at atmospheric pressure) strength with a clinical scanner, highlighting the need for further investigation. Note that previously we have shown through numerical investigation that subharmonic response can theoretically increase or decrease with overpressure depending on the ratio of the natural frequency of the microbubble, which is a function of the ambient pressure, to the excitation frequency [34]. We showed that the subharmonic response attains a maximum when this ratio between frequencies is a critical value close to ~0.5. Increasing overpressure increases the natural frequency and, thereby, its ratio to the excitation frequency, moving it either toward the critical value (increasing the subharmonic) or away from it (decreasing the subharmonic).

For SonoVue with its Type I and Type II subharmonics, we found the SHAPE sensitivity trend was different from other bubbles with perfluorocarbon gas core [30]. Specifically, while the Type II subharmonic response of SonoVue bubbles (i.e., at very high acoustic pressures) was typical of the one seen in the growth-saturation stage of other bubbles, the Type I subharmonic, at low PNPs, was present at atmospheric pressure only for SonoVue bubbles. During pressurization-depressurization cycles, it was present in earlier cycles with its amplitude decreasing with overpressure. For later cycles, it disappeared at atmospheric pressure to appear under overpressure, this behavior being identical to our previous in-house PFB bubbles [32].

Kanbar et al. [35] showed that bubbles with cores of air or SF_6 with higher diffusivity than perfluorocarbons (PFC) exhibit subharmonic signals at 10 MHz acoustic excitations of 450 kPa, whereas bubbles with a PFC gas core produced subharmonic signals only after a 20–40 min delay. This observation was related to the quick outward diffusion of air or SF_6 that creates a buckled shell and compression-only behavior that was associated with subharmonic generation [36–38]. Similarly, Shekhar et al. [39] showed that altering the diffusion rate by adjusting the air saturation level of the surrounding medium affects the subharmonic production, where bubbles in media with higher air saturation levels hence, lower diffusion rates, showed a delayed onset of subharmonic signal generation.

We think that the Type I subharmonic of SonoVue observed at unusually low excitation amplitudes 30 is due to bubble shrinkage and buckling caused by outward SF_6 diffusion. Here, we investigate the role of the gas core on the subharmonic response of SonoVue and its sensitivity to ambient pressure, by switching the SF_6 core with a lower diffusivity C_4F_{10} (perfluorobutane [PFB]) gas. For the rest of the paper, we refer to SonoVue with PFB as SonoVuePFB, and the control case, reformulating by taking SF_6 out and putting it back, as SonoVueR. We studied the acoustic response and subharmonic production at the atmospheric pressure and overpressures ranging from 5 to 25 kPa (37–186 mm Hg) over a PNP range of 25–700 kPa. Due to the large number of parameters, we restricted here to a single frequency which is representative of the resonance frequency of the polydisperse SonoVue agent as reported in the literature [25,40,41]. The pressure sensitivity of subharmonic response at different frequencies was studied previously [32] resulting in qualitatively similar behaviors.

Methods

SonoVue with PFB core

Before activating SonoVue bubbles as instructed in the product manual, the headspace of the vial containing SF_6 was removed using a needle connected to the vacuum outlet. After vacuuming the headspace for two minutes (which created a -20 kPa pressure inside the vial), it was connected to a pressure-regulated PFB cylinder (FlouroMed L.P., Round Rock, TX, USA) and filled up until 5 kPa pressure was reached inside the vial. The next steps were based on the original activation protocol for SonoVue with SF_6 in the head space. Briefly, 5 mL saline water was injected and the vial was shaken by hand for 20 seconds. The resultant solution containing SonoVuePFB was used within two hours of activation. To investigate the effects of SF_6 removal, we also reformulated a control case of SonoVueR by drawing 5 mL SF_6 out of the headspace of a SonoVue vial using an injection syringe and then immediately replacing it with more SF_6 (making sure to reach 5 kPa pressure in the vial as in the case of SonoVuePFB).

Microbubble size measurement

To compare the size distribution of SonoVue, SonoVueR, and SonovuePFB, optical microscopy was used to measure the size distributions. In a similar setup and procedure to Azami et al. [42], a 10 μL aliquot of 11 times diluted bubble suspension was injected into a hemocytometer counting chamber. An in-house MATLAB (Mathworks, Natick, MA, USA) image processing program was used to count bubbles over 12 optical microscopy images taken at 40x magnification from random locations in the counting chamber. This procedure was replicated three times to calculate the average size distribution from a population of more than 4000 bubbles ($n = 3$). The polydispersity of the size distributions was quantified by calculating the polydispersity index (PDI), which is the ratio of the standard deviation of the size distribution to the mean size.

Pressure-dependent scattering setup

The acoustic responses of various bubbles under varying static ambient pressures were measured using the pressurizing chamber and the acoustic measurement tank described in detail in our previous papers [32]. For each experiment, 140 mL of 1000 (2000) times diluted SonoVue (SonoVuePFB) suspension was transferred into the pressurizing chamber before placing it inside an acoustic measurement tank filled with deionized water as shown in Figure 1a. The difference in concentration was in response to higher attenuation by SonoVuePFB (See Fig. 2a below) and based on preliminary experimental observations to obtain sufficient sensitivity for the SonoVuePFB scattering experiments. A calibrated 5 MHz focused transducer (V309, Olympus, Waltham, MA, USA) was driven by arbitrary function generator (DG1022, RIGOL, Portland, OR, USA) through a 55 dB linear power amplifier (A150, E&I, Rochester, NY, USA) to transmit acoustic excitations at 3 MHz frequency and 25–700 kPa peak negative pressure (PNP) into the pressurizing chamber. The sinusoidal ultrasound pulse consisted of 32 cycles and the repetition frequency was 100 Hz. The scattered acoustic response from the bubble suspension inside the pressure chamber was received by a broadband focused transducer (Y-102, Sonic Concepts, Bothell, WA, USA; -6 dB bandwidth of 10 kHz–15 MHz, 19 mm active diameter, and 50 mm geometric focal length). The received signal was filtered and amplified 20 dB by an ultrasonic pulser/receiver (Model 5800, Panametrics, Olympus, Waltham, MA, USA) and fed into an oscilloscope (MDO 3024, Tektronix, Beaverton, OR, USA). A MATLAB program was used to record twenty voltage time signals from the oscilloscope in sample mode. The averaged power spectrum was calculated offline using a Fast Fourier Transform with 1 V amplitude taken as the reference signal amplitude for calculations in dB.

Experimental procedure for pressure-dependent scattering measurement

The acoustic response of the bubbles was measured under static pressurization-depressurization cycles as described previously [30]. During each experiment, the pressure inside the chamber was increased to the same value and released eight times keeping the acoustic excitation constant. In each of the eight pressurization-depressurization cycles, the acoustic response was measured once immediately before pressurization (i.e., at atmospheric pressure) and once at the fixed overpressure, as described in Figure 1b. For each parameter combination of 9 different PNPs (25–700 kPa) and 5 different ambient overpressures (5, 10, 15, 20, or 25 kPa), a fresh suspension of bubbles was used. Each measurement lasted for 210 ± 10 seconds. The experiments were replicated three times.

Attenuation setup

Attenuation was used to assess the effects of gas removal from the SonoVue vial during the gas exchange by comparing attenuation through SonoVue and SonoVueR following methods described in our previous publications [42,43,44]. Briefly, 1 ml of microbubble suspension was diluted with 1950 ml of deionized (DI) water in a polycarbonate chamber. A magnetic stirrer was used to ensure the microbubbles were uniformly distributed during the measurements. The same pulser-receiver as in the scattering setup was used in a pulse-echo mode to transmit and receive pulses through a 5 MHz single element (-6 dB bandwidth: 2.8–6.4 MHz) unfocused transducer (V309, Olympus, Waltham, MA, USA) with a 100 Hz pulse repetition frequency (PRF). An external attenuator with an 11 dB setting was turned on to ensure negligible nonlinear dynamics. The oscilloscope received the signal with a 73 μs delay and a 1.5 GHz sampling rate in 64 sequence average mode. Signals were recorded as described in the previous section. Each measurement was repeated at least four times. Signals were recorded before and after the microbubble injection as shown in Figure 1c. The fast Fourier transform (FFT) of the recorded signals was taken to calculate attenuation coefficients (dB/cm) as:

$$\alpha(\omega) = 10\log\left(V^2{}_c(\omega)/V^2{}_{MB}(\omega)\right)/d$$

Where V_{MB} and V_c are the received signals in the frequency with and without microbubbles, respectively, and d is the distance from the transducer face to the back wall of the chamber.

Results and discussion

To investigate the effects of gas removal during gas exchange, attenuation was compared between SonoVue and SonoVueR in Figure 2a and showed very little difference, i.e., no effect on the constitution and

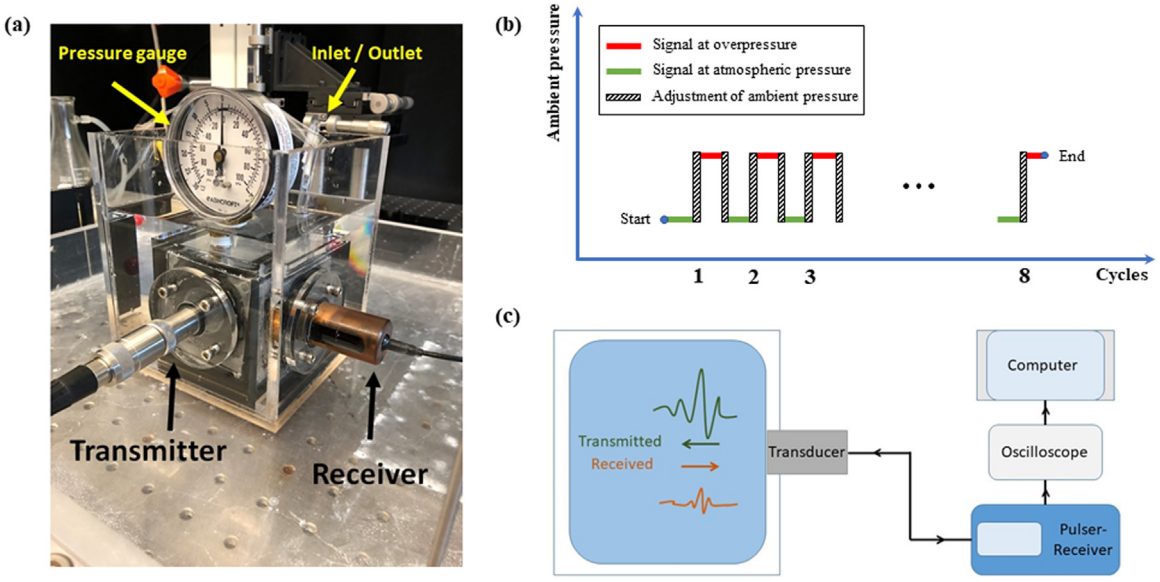

Figure 1. (a) Acoustic measurement tank with two transducers embedded in the wall. A pressurizing chamber was placed inside the tank and an air syringe was used to adjust the pressure inside the chamber. (b) Recording sequence of pressurization-depressurization cycles. (c) Acoustic attenuation setup with a 5 MHz unfocused transducer. The water tank was initially filled with DI water. Recordings were done with and without microbubbles to measure the attenuation of microbubbles.

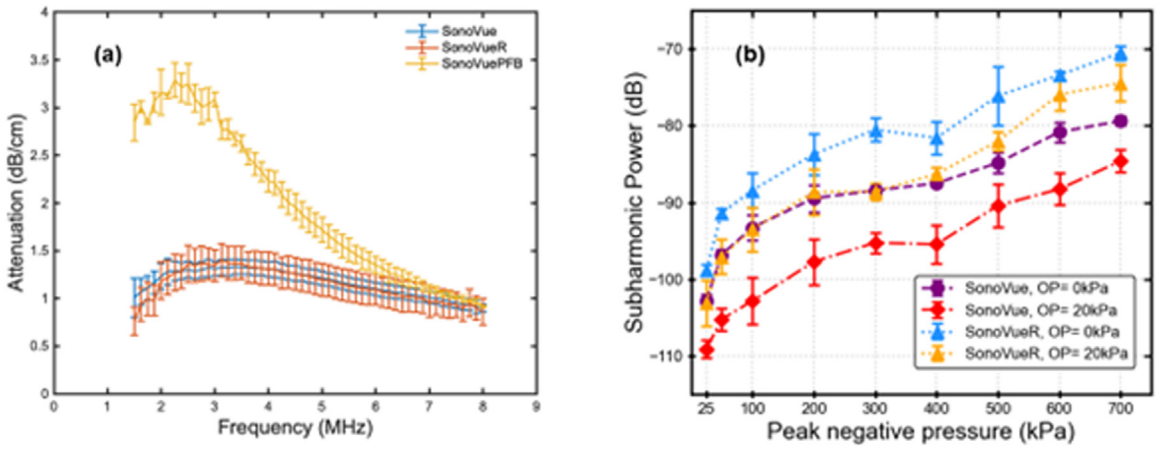

Figure 2. (a) Frequency-dependent attenuation of SonoVue, SonoVueR, and SonoVuePFB. (b) Subharmonic responses from SonoVue and SonoVueR as a function of PNP at atmospheric (0 kPa) and 20 kPa overpressure in the first cycle.

thereby the dynamics of microbubbles due to removing the SF_6 and inserting it back. However, SonoVuePFB presented a significantly higher response than those two. As will be seen below, they all have very similar size distributions. Therefore, the difference can only be attributed to the shell properties, caused by the different gas cores and their different diffusivities—substantially lower for SF_6 than perfluorobutane. The subharmonic response depicted in Figure 2b shows that responses both at atmospheric pressure and at 20 kPa overpressure experienced an increase with a parallel shift of the curves for SonoVueR compared to for SonoVue. However, this translates to no difference in the SHAPE response which is a relative measure [30].

The acoustic responses from SonoVue and SonovuePFB are shown in Figure 3. Unlike SonoVue, SonoVuePFB does not show subharmonic generation at low acoustic excitations (Fig. 3a), the latter behavior being more typical. Figure 3b and c show the frequency responses of SonoVuePFB as well as SonoVue to a low (100 kPa) and a high (600 kPa) acoustic excitation, respectively. The response at 100 kPa excitation shows a sharp contrast due to the gas core exchange; while spectra due to both bubbles consist of fundamental, second harmonic, and a very low amplitude third harmonic, a significant subharmonic peak is present only for SonoVue. Previously, we saw a strong subharmonic response even at 25 kPa excitation [30] (Fig. 2b). This indicates that the gas core has a significant effect on the bubble dynamic. The high diffusivity of SF_6 makes SonoVue buckle due to gas egress leading to subharmonic generation. With a PFB gas core, due to its lower diffusivity, the bubble might retain its original volume and an unbuckled elastic condition resulting in no subharmonic. Note that other researchers also observed SF_6 and air bubbles to be more prone to generate subharmonic signals compared to the ones with PFC gas cores [35].

Size distribution has been shown to affect the subharmonic response of microbubbles as a function of excitation and overpressure [45–47]. To investigate the effects of gas exchange on microbubble production and the resultant size distribution, we compared the size distributions of SonoVue, SonoVueR, and SonoVuePFB in Figure 4a immediately after activation. SonoVue and SonoVueR showed very similar distributions indicating negligible effects due to the process of removing SF_6 from the vial and replacing it with SF_6. SonoVuePFB consisted of smaller bubbles than the other two. However, all had a very similar mean diameter: 2.5 $\pm$ 0.03 μm (PDI = 0.64), 2.48 $\pm$ 0.04 μm (PDI = 0.64), and 2.37 $\pm$ 0.03 μm (PDI = 0.66) for SonoVue, SonoVueR, and SonoVuePFB respectively. The average concentrations were also similar: 5.56 $\pm$ 0.09 $\times$ 10^8 per ml (SonoVue), 5.28 $\pm$ 0.97 $\times$ 10^8 per ml (SonoVueR) (both within the range

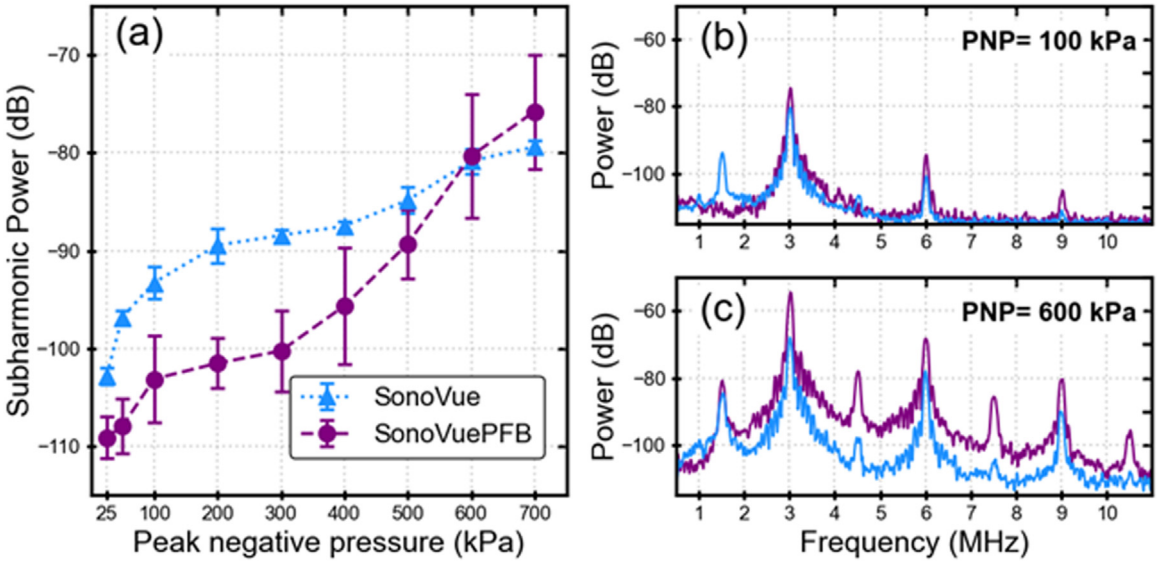

Figure 3. (a) Subharmonic responses from SonoVue and SonoVuePFB as functions of PNP. (b) and (c) Plot the corresponding frequency spectra to acoustic PNP of 100 and 600 kPa, respectively.

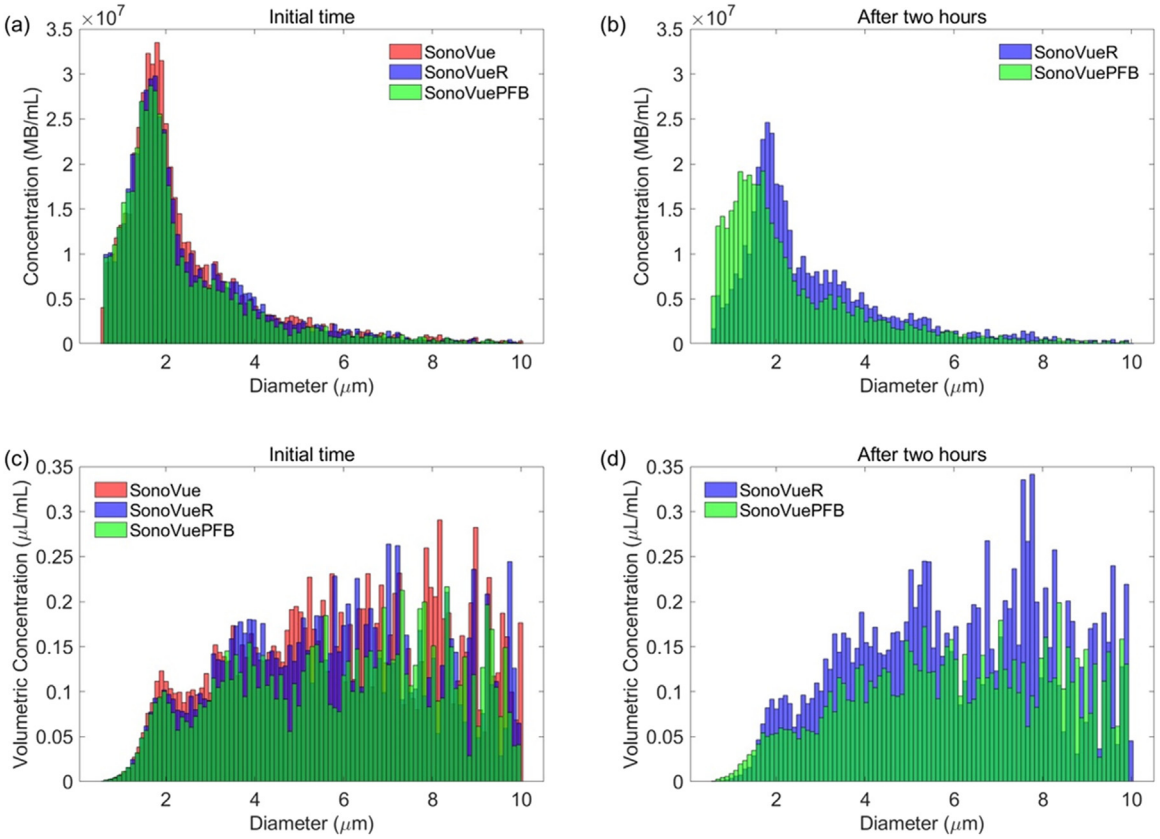

Figure 4. Size distribution of SonoVue, SonoVueR, and SonovuePFB microbubbles (a) immediately after activation and (b) after 2 hours. (c) and (d) are corresponding volume distributions.

reported by the manufacturer), $4.74 \pm 0.43 \times 10^8$ per ml (SonoVuePFB). The volume concentrations for SonoVue, SonoVueR, and SonoVuePFB were 12.75 ± 1.48, 11.55 ± 1.78, and 9.77 ± 1.48 μl/ml, respectively. To estimate the stability of the bubbles, in Figure 5b we plot the size distribution 2 hours after activation (shelf life according to the vendor) recording diameters and concentrations as 2.86 ± 0.13 μm (PDI = 0.60) and $4.25 \pm 0.07 \times 10^8$ for SonoVueR and 2.37 ± 0.15 μm (PDI = 0.70) and $3.97 \pm 1.1 \times 10^8$ for SonoVuePFB. The mean size remains similar over the period with an extremely small decrease in concentration possibly due to coalescence.

In Figure 5, the effects of applying 20 kPa overpressure on the acoustic response bubbles at a low (100 kPa), an intermediate (400 kPa), and a high (600 kPa) PNP are shown. Figure 5a reveals that applying 20 kPa overpressure led to a more than 20 dB increase in subharmonic response (peak at 1.5 MHz) of SonoVuePFB at 100 kPa excitation amplitude. In Figure 5b, we demonstrate that this increase in subharmonic response is consistent in magnitude during the eight cycles of pressurizing in sharp contrast to native SonoVue, where the baseline subharmonic at zero overpressure declines to noise level after undergoing multiple cycles of pressurizing-depressurizing cycles. The subharmonic for native SonoVue at the first cycle records a decrease and then an increase in subsequent cycles. The magnitude of increase in subharmonic for SonoVuePFB is significantly higher than SonoVue and previous studies of C_4F_{10} bubbles, which recorded a maximum increase of less than 15 dB [30,32]. Figure 5c shows a similar behavior at 400 kPa PNP, in that almost no distinguishable subharmonic at atmospheric pressure gives rise to a subharmonic peak at 20 kPa overpressure. In Figure 5e, at a high PNP of 600 kPa, there is subharmonic at atmospheric pressure as one would expect. However, applying overpressure further increases the subharmonic. Figure 5b, d, and f demonstrate the consistency of the subharmonic presence of SonoVuePFB (in contrast to native SonoVue) and its increase with overpressure over eight cycles. Additionally, we note that the baseline subharmonic at atmospheric pressure remains unchanged for SonoVuePFB, signaling the stability of the PFB core bubbles against ambient hydrostatic pressures (Fig. 5b, d, and f). The increase in subharmonic at the higher PNPs (>400 kPa) is in contrast with all previous experimental studies where an increase in subharmonic was only reported for low excitation amplitudes. The traditional Type II subharmonic at higher PNPs (>400 kPa) decreased with overpressure [30,32]. The atypical behavior of SonoVuePFB warrants further investigation. Other ultra-harmonics experience a decrease.

The ambient pressure sensitivity of SonoVuePFB bubbles averaged over 8 cycles of pressurization and three replications ($n = 3$) is shown in Figure 6. They show a monotonic increase with overpressure up to 20 kPa and then a decrease to 25 kPa. The pressure sensitivity of SonoVuePFB in the interval 0−20 kPa averaged over eight cycles is reported in Table 1. It was compared with the sensitivity of native SonoVue only in the first cycle as the response changed over multiple pressurization-depressurization cycles. We observe that, unlike previous studies of SF_6-SonoVue and C_4F_{10} lipid bubbles, here the sensitivity correlation is always positive. However, as the excitation PNP rises, above the typical threshold value (PNP > 400 kPa) the slope of the correlation declines. Xu et al. [27] also saw subharmonic decreases with overpressure for PNP > 480 kPa. Kalayeh et al [48] too observed a decrease in Lumason subharmonic response with overpressure at the growth stage. Also, as was seen by previous observers [27,29,31] a triphasic behavior is seen with an overpressure increase, i.e., it initially increases, then reaches a plateau and subsequently decreases.

Figure 7 compares the subharmonic curve as a function of PNP obtained at 20 kPa overpressure to the ones at atmospheric pressure shown in Figure 3a. The SonoVuePFB subharmonic curve at 20 kPa overpressure exhibits a similar profile to SonoVue at atmospheric pressure, generating significant subharmonic at low acoustic excitations. The

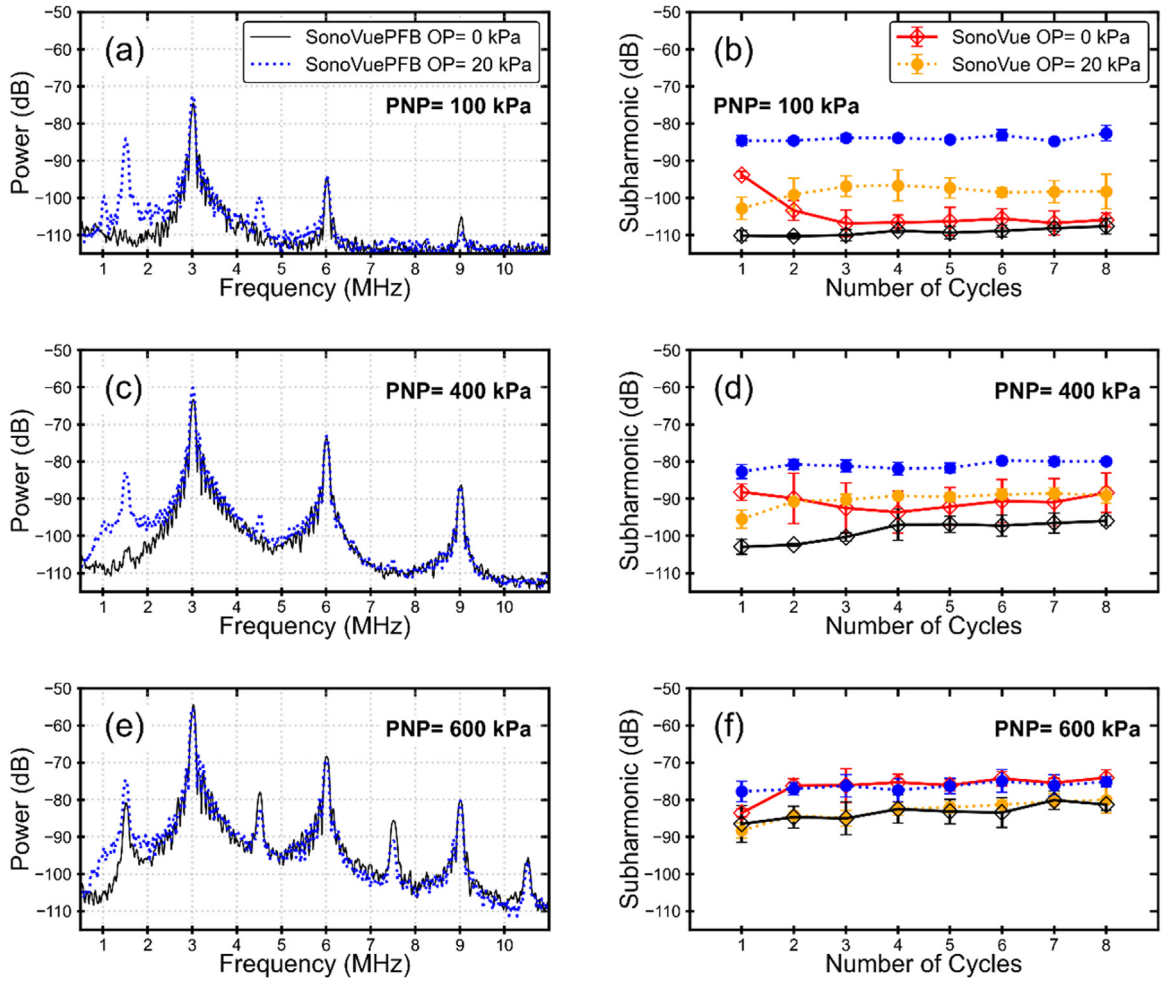

Figure 5. Acoustic response of SonoVuePFB bubbles at atmospheric pressure and 20 kPa overpressure at (a) 100 kPa, (c) 400 kPa, and (e) 600 kPa PNP. The effect of overpressure during the 8 cycles of pressurization-depressurization (atmospheric and 20 kPa) at (b) 100 kPa, (d) 400 kPa, and (f) 600 kPa PNP for SonoVue and SonoVue PFB.

SonoVuePFB subharmonic profile at other overpressure values exhibits the same feature but is not shown here for brevity.

The similarity between the subharmonic curve of a pressurized (20 kPa) bubble with a PFB gas core and SonoVue with an SF_6 core at atmospheric pressure seen in Figure 7 implies a similarity in mechanism between the two: a buckled state. Based on the findings by Frinking et al. [28] and Sijl et al. [36] bubbles in a buckled state undergo compression-only behavior and enhanced subharmonic production. For

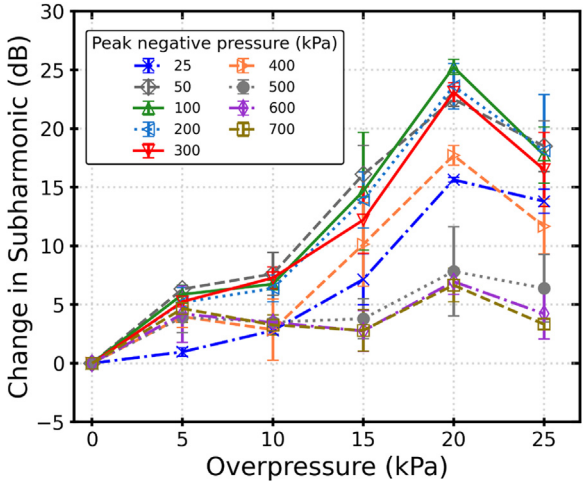

Figure 6. Ambient pressure sensitivity of subharmonic response. PFB SonoVue shows a positive correlation between overpressure and subharmonic amplitude.

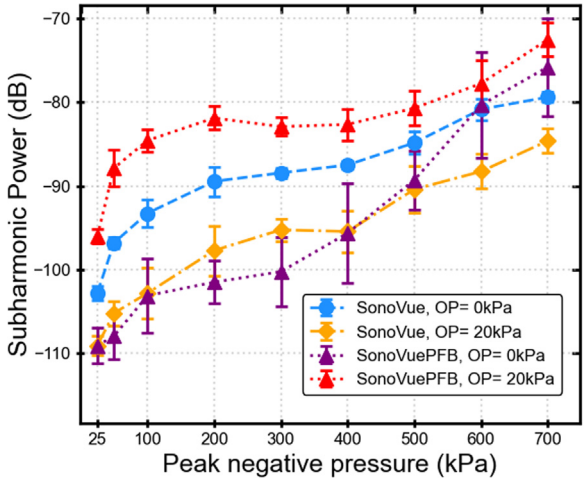

Figure 7. Comparison of subharmonic curves as a function of acoustic peak negative pressure (PNP) for SonoVuePFB and SonoVue with and without 20 kPa overpressure.

SonoVue, due to the higher diffusivity of SF_6 even at atmospheric pressure bubbles shrink to a buckled state due to gas loss, whereas for SonoVuePFB, due to the lower diffusivity of its gas, only an ambient pressure increase (20 kPa) leads to gas loss and buckling. Once the bubble is buckled either due to gas diffusion at atmospheric pressure and shrinkage (SonoVue at high PNPs) or due to gas diffusion upon overpressure (SonoVuePFB, at low PNPs and overpressures of 10–15 kPa), we observe that further increase in overpressure leads to saturation and decrease in subharmonic. This manifested in the tri-phasic profile of subharmonic increase at low PNPs and a general decrease in subharmonic with overpressure at high enough PNPs, as widely noted in the literature. An exception to the latter is the consistent increase in subharmonic response by overpressure at high PNP in this study for the SonoVuePFB bubbles. Although it still shows a tri-phasic increase, further study is needed to investigate the effect of other possible parameters such as microbubble concentration.

The high magnitude of increase in low excitation subharmonic in this study suggests a strong potential for SHAPE applications. While one drawback is the low amplitude of subharmonic at low excitations and the difficulty in signal detection, the more than 20 dB increase in the signal amplitude should put the subharmonic amplitude into a detectable level. However, Mayer et al. [31] recently investigated *in vitro* SHAPE performance of SonoVue, Sonazoid, and Definity below the subharmonic threshold stage but did not observe any subharmonic appearance with overpressure. Further investigation of the overpressure effects on subharmonic generation below the subharmonic threshold is warranted.

Data availability

The data sets generated and/or analyzed during the current study are available from the corresponding author upon reasonable request.

Acknowledgment

K.S., F.F., and J.R.E. acknowledge partial support from the National Institutes of Health Award R01 EB032333. K.S. acknowledges partial support from National Science Foundation Award 1239105.

Conflict of interest

The authors declare no competing interests.

References

[1] Sontum PC. Physicochemical characteristics of Sonazoid, a new contrast agent for ultrasound imaging. Ultrasound Med Biol 2008;34(5):824–33.
[2] Frinking P, Segers T, Luan Y, Tranquart F. Three decades of ultrasound contrast agents: a review of the past, present and future improvements. Ultrasound Med Biol 2020;46(4):892–908.
[3] Stride E, Segers T, Lajoinie G, Cherkaoui S, Bettinger T, Versluis M, et al. Microbubble agents: new directions. Ultrasound Med Biol 2020;46(6):1326–43.
[4] de Jong N, Bouakaz A, Frinking P. Basic acoustic properties of microbubbles. Echocardiography 2002;19(3):229–40.
[5] Helfield B. A review of phospholipid encapsulated ultrasound contrast agent microbubble physics. Ultrasound Med Biol 2019;45(2):282–300.
[6] Shi WT, Forsberg F. Ultrasonic characterization of the nonlinear properties of contrast microbubbles. Ultrasound Med Biol 2000;26(1):93–104.
[7] Ferrara K, Pollard R, Borden M. Ultrasound microbubble contrast agents: fundamentals and application to gene and drug delivery. Annu Rev Biomed Eng 2007;9:415–47.
[8] Fix SM, Borden MA, Dayton PA. Therapeutic gas delivery via microbubbles and liposomes. J Control Release 2015;209:139–49.
[9] Salib A, Halpern E, Eisenbrey J, Chandrasekar T, Chung PH, Forsberg F, et al. The evolving role of contrast-enhanced ultrasound in urology: a review. World J Urol 2023;41(3):673–8.
[10] Forsberg F, Piccoli CW, Sridharan A, Wilkes A, Sevrukov A, Ojeda-Fournier H, et al. 3D Harmonic and subharmonic imaging for characterizing breast lesions: a multicenter clinical trial. J Ultrasound Med 2022;41(7):1667–75.
[11] Eisenbrey JR, Sridharan A, Liu JB, Forsberg F. Recent experiences and advances in contrast-enhanced subharmonic ultrasound. Biomed Res Int 2015;2015:640397.
[12] Eisenbrey JR, Forsberg F. Contrast-enhanced ultrasound for molecular imaging of angiogenesis. Eur J Nucl Med Mol Imaging 2010;37(Suppl. 1):S138–46.
[13] Malone CD, Fetzer DT, Monsky WL, Itani M, Mellnick VM, Velez PA, et al. Contrast-enhanced US for the interventional radiologist: current and emerging applications. Radiographics 2020;40(2):562–88.
[14] Forsberg F, Stanczak M, Sinanan JK, Blackman R. Second-generation differential tissue harmonic imaging improves the visualization of renal lesions. J Ultrasound Med 2022;42:853–7.
[15] Forsberg F, Liu JB, Shi WT, Furuse J, Shimizu M, Goldberg BB. In vivo pressure estimation using subharmonic contrast microbubble signals: proof of concept. IEEE Trans Ultrason Ferroelectr Freq Control 2005;52(4):581–3.
[16] Dave JK, Halldorsdottir VG, Eisenbrey JR, Liu JB, McDonald ME, Dickie K, et al. Noninvasive estimation of dynamic pressures in vitro and in vivo using the subharmonic response from microbubbles. IEEE Trans Ultrason Ferroelectr Freq Control 2011;58(10):2056–66.
[17] Dave JK, Halldorsdottir VG, Eisenbrey JR, Raichlen JS, Liu JB, McDonald ME, et al. Noninvasive LV pressure estimation using subharmonic emissions from microbubbles. JACC Cardiovasc Imag 2012;5(1):87–92.
[18] Dave JK, Kulkarni SV, Pangaonkar PP, Stanczak M, McDonald ME, Cohen IS, et al. Non-invasive intra-cardiac pressure measurements using subharmonic-aided pressure estimation: proof of concept in humans. Ultrasound Med Biol 2017;43(11):2718–24.
[19] Gupta I, Eisenbrey JR, Machado P, Stanczak M, Wessner CE, Shaw CM, et al. Diagnosing portal hypertension with noninvasive subharmonic pressure estimates from a US contrast agent. Radiology 2021;298(1):104–11.
[20] Esposito C, Machado P, McDonald ME, Savage MP, Fischman D, Mehrotra P, et al. Noninvasive evaluation of cardiac chamber pressures using subharmonic-aided pressure estimation with definity microbubbles. JACC Cardiovasc Imag 2023;16(2):224–35.
[21] Andersen KS, Jensen JA. Impact of acoustic pressure on ambient pressure estimation using ultrasound contrast agent. Ultrasonics 2010;50(2):294–9.
[22] Sarkar K, Shi WT, Chatterjee D, Forsberg F. Characterization of ultrasound contrast microbubbles using *in vitro* experiments and viscous and viscoelastic interface models for encapsulation. J Acoust Soc Am 2005;118(1):539–50.
[23] Helfield BL, Cherin E, Foster FS, Goertz DE. Investigating the subharmonic response of individual phospholipid encapsulated microbubbles at high frequencies: a comparative study of five agents. Ultrasound Med Biol 2012;38(5):846–63.
[24] Shi W, Forsberg F, Raichlen J, Needleman L, Goldberg B. Pressure dependence of subharmonic signals from contrast microbubbles. Ultrasound Med Biol 1999;25(2):275–83.
[25] Kaushik A, Khan AH, Pratibha DSV, Shekhar H. Effect of temperature on the acoustic response and stability of size-isolated protein-shelled ultrasound contrast agents and SonoVue. J Acoust Soc Am 2023;153(4):2324.
[26] Biagi E, Breschi L, Vannacci E, Masotti L. Stable and transient subharmonic emissions from isolated contrast agent microbubbles. IEEE Trans Ultrason Ferroelectr Freq Control 2007;54(3):480–97.
[27] Xu G, Lu H, Yang H, Li D, Liu R, Su M, et al. Subharmonic scattering of SonoVue microbubbles within 10-40-mmHg overpressures in vitro. IEEE Trans Ultrason Ferroelectr Freq Control 2021;68(12):3583–91.
[28] Frinking PJ, Brochot J, Arditi M. Subharmonic scattering of phospholipid-shell microbubbles at low acoustic pressure amplitudes. IEEE Trans Ultrason Ferroelectr Freq Control 2010;57(8):1762–71.
[29] Nio AQX, Faraci A, Christensen-Jeffries K, Raymond JL, Monaghan MJ, Fuster D, et al. Optimal control of SonoVue microbubbles to estimate hydrostatic pressure. IEEE Trans Ultrason Ferroelectr Freq Control 2020;67(3):557–67.
[30] Azami RH, Forsberg F, Eisenbrey JR, Sarkar K. Acoustic response and ambient pressure sensitivity characterization of SonoVue for noninvasive pressure estimation. J Acoust Soc Am 2024;155(4):2636–45.
[31] Mayer H, Kim GW, Machado P, Eisenbrey JR, Wallace K, Forsberg F. Investigation into the subharmonic response of three contrast agents in static and dynamic flow environments using a commercially available diagnostic ultrasound scanner. Ultrasound Med Biol 2024;50(11):1731–8.
[32] Azami RH, Forsberg F, Eisenbrey JR, Sarkar K. Ambient pressure sensitivity of the subharmonic response of coated microbubbles: effects of acoustic excitation parameters. Ultrasound Med Biol 2023;49(7):1550–60.
[33] Dave JK, Halldorsdottir VG, Eisenbrey JR, Merton DA, Liu JB, Machado P, et al. On the implementation of an automated acoustic output optimization algorithm for subharmonic aided pressure estimation. Ultrasonics 2013;53(4):880–8.
[34] Katiyar A, Sarkar K, Forsberg F. Modeling subharmonic response from contrast microbubbles as a function of ambient static pressure. J Acoust Soc Am 2011;129(4):2325–35.
[35] Kanbar E, Fouan D, Sennoga CA, Doinikov AA, Bouakaz A. Impact of filling gas on subharmonic emissions of phospholipid ultrasound contrast agents. Ultrasound Med Biol 2017;43(5):1004–15.
[36] Sijl J, Overvelde M, Dollet B, Garbin V, de Jong N, Lohse D, et al. "Compression-only" behavior: a second-order nonlinear response of ultrasound contrast agent microbubbles. J Acoust Soc Am 2011;129(4):1729–39.
[37] Sijl J, Dollet B, Overvelde M, Garbin V, Rozendal T, de Jong N, et al. Subharmonic behavior of phospholipid-coated ultrasound contrast agent microbubbles. J Acoust Soc Am 2010;128(5):3239–52.
[38] Prosperetti A. A general derivation of the subharmonic threshold for non-linear bubble oscillations. J Acoust Soc Am 2013;133(6):3719–26.
[39] Shekhar H, Awuor I, Thomas K, Rychak JJ, Doyley MM. The delayed onset of subharmonic and ultraharmonic emissions from a phospholipid-shelled microbubble contrast agent. Ultrasound Med Biol 2014;40(4):727–38.
[40] Li F, Li D, Yan F. Improvement of detection sensitivity of microbubbles as sensors to detect ambient pressure. Sensors (Basel) 2018;18(12):4083.

[41] Greis C. Technology overview: SonoVue (Bracco, Milan). Eur Radiol 2004;14(Suppl. 8):P11–5.
[42] Azami RH, Aliabouzar M, Osborn J, Kumar KN, Forsberg F, Eisenbrey JR, et al. Material properties, dissolution and time evolution of PEGylated lipid-shelled microbubbles: effects of the PEG hydrophilic chain configurations. Ultrasound Med Biol 2022; 48(9):1720-1732.
[43] Chatterjee D, Sarkar K, Jain P, Schreppler NE. On the suitability of broadband attenuation measurement for characterizing contrast microbubbles. Ultrasound Med Biol 2005;31(6):781–6.
[44] Paul S, Russakow D, Rodgers T, Sarkar K, Cochran M, Wheatley MA. Determination of the interfacial rheological properties of a Poly(DL-lactic acid)-encapsulated contrast agent uning in vitro attenuation and scattering. Ultrasound Med Biol 2013;39(7):1277–91.
[45] Katiyar A, Sarkar K, Forsberg F. Modeling subharmonic response from contrast microbubbles as a function of ambient static pressure. J Acoust Soc Am 2011;129 (4):2325–35.
[46] Katiyar A, Sarkar K. Excitation threshold for subharmonic generation from contrast microbubbles. J Acoust Soc Am 2011;130(5):3137–47.
[47] Katiyar A, Sarkar K. Effects of encapsulation damping on the excitation threshold for subharmonic generation from contrast microbubbles. J Acoust Soc Am 2012;132 (5):3576–85.
[48] Kalayeh K, Fowlkes JB, Yeras S, Chen A, Daignault-Newton S, Schultz WW. A comparative study of commercially available ultrasound contrast agents for sub-harmonic-aided pressure estimation (SHAPE) in a bladder phantom. Ultrasound Med Biol 2024;50:1494–505.